*Journal of Statistical Physics, Vol. 80, Nos. 1/2, 1995*

# Self-Avoiding Walks on Random Fractal Environments

**Yossi Shussman**[1] **and Amnon Aharony**[1]

*Received September 22, 1994; final December 30, 1994*

Self-avoiding random walks (SAWs) are studied on several hierarchical lattices in a randomly disordered environment. An analytical method to determine whether their fractal dimension $D_{saw}$ is affected by disorder is introduced. Using this method, it is found that for some lattices, $D_{saw}$ is unaffected by weak disorder; while for others $D_{saw}$ changes even for infinitesimal disorder. A weak disorder exponent $\lambda$ is defined and calculated analytically [$\lambda$ measures the dependence of the variance in the partition function (or in the effective fugacity per step) $v \sim L^{\lambda}$ on the end-to-end distance of the SAW, $L$]. For lattices which are stable against weak disorder ($\lambda < 0$) a phase transition exists at a critical value $v = v^*$ which separates weak- and strong-disorder phases. The geometrical properties which contribute to the value of $\lambda$ are discussed.

**KEY WORDS:** Self-avoiding walks; disordered environment; hierarchical lattices; fractals; renormalization.

## 1. INTRODUCTION

In this paper we discuss the statistics of self-avoiding random walks (SAWs) in a quenched random environment. SAWs are often used as a model of polymer chains[1] and therefore SAWs on a random environment represent polymers in realistic media. The problem of SAWs in a quenched random environment is nontrivial, and both the significance and the complexity of the problem have caused it to attract much attention in the last decade.

In a pure (i.e., deterministic and nonrandom) environment, where all the steps are identical to each other and associated with the same energy, the SAW average length $\bar{N}$ scales as a power law $\bar{N} \sim L^D$, where the walk has an end-to-end Euclidean distance $L$ (both of its ends are fixed at a distance $L$ apart) and $D$ is the SAW fractal dimension (the fractal dimension

[1] School of Physics and Astronomy, Raymond and Beverly Sackler Faculty of Exact Sciences, Tel Aviv University, Ramat Aviv 69978, Israel.



0022-4715/95/0700-0147$07.50/0 

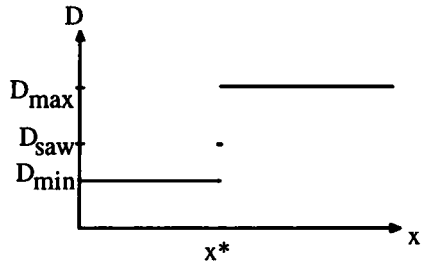


Fig. 1. Dependence of the SAW's fractal dimension $D$ on the fugacity $x$.

$D$ is sometimes represented by a size exponent $\nu$, $D = 1/\nu$). Due to this definition of $D$, the length average is performed on a grand-canonical ensemble of SAWs with equal linear sizes $L$ and different numbers of steps $N$. In this ensemble, each step is associated with a fugacity weight factor denoted by $x$. It is straightforward to show[2, 3] that in a nonrandom fractal environment $D$ depends on the type of the lattice and on the value of the fugacity $x$ (Fig. 1). There is a critical value $x_c$ below which the SAW is in a stretched phase, while above it it is in a compact phase. In these phases, the SAW has the fractal dimension $D = D_{max}$ or $D = D_{min}$, respectively ($D_{max}$ and $D_{min}$ are the dimensions of the maximum- and the minimum-length SAWs on the lattice, respectively). The case which represents the nontrivial behavior of SAWs is when $x = x_c$, where the SAW has a fractal dimension $D = D_{saw}$.

In a random environment, it is much more difficult to obtain the properties of the average-length SAW. One of the interesting questions regarding this issue concerns the conditions under which an initial weak disorder increases or decays under coarse graining to larger units. This question was discussed by Le Doussal and Machta[4]. Using Monte Carlo simulations on several hierarchical structures, they concluded that for hierarchical lattices which can be embedded on Euclidean lattices with a sufficiently low dimensionality, weak disorder is always relevant, i.e., its effects increase as the system's linear size $L$ grows. For more multiply connected hierarchical structures, which exist only on Euclidean lattices with high dimensions, they found a phase transition between a weak-disorder phase and a strong-disorder phase: if the disorder is weak, its effects decay as $L$ grows, and thus on large length scales the SAW behaves as if its environment was nonrandom. On the other hand, if the disorder is strong, its effects increase as $L$ grows.

In this paper, we introduce an algorithm which uses the real-space renormalization-group (RSRG) approach to obtain recursion relations

for the positive integer moments $\langle Z^k \rangle$ of the SAW partition function (equivalent to the effective renormalized fugacity per step) on various hierarchical lattices. Having these recursion relations, we are able to conclude analytically whether a weak-disorder–strong-disorder transition occurs for each one of those lattices. We also introduce a weak-disorder crossover exponent $\lambda$ which measures the growth or the decay of an initially weak disorder as a function of the lattice linear size $L$.

The outline of this paper is as follows: In Section 2 we introduce the studied fractals. Section 3 presents the RSRG, which is the analytical method used in this paper. In Section 4 we discuss the growth or decay of an initial disorder, introduce the weak-disorder decay exponent defined via the size dependence of the variance of the distribution of the partition function, and identify the conditions for the existence of a weak-disorder–strong-disorder transition. Section 5 generalizes the discussion to higher cumulants of the partition function, and Section 6 summarizes the conclusions and presents a discussion.

## 2. THE FRACTALS

We chose to study the behavior of the SAWs in a random environment on seven lattice structures. Two stages of the iterative construction of these fractals are presented in Fig. 2. The first lattice (Fig. 2a) is the one-dimensional lattice, which is studied here only for didactic purposes. The second lattice is the Mandelbrot–Given curve (Fig. 2b), which is often used to imitate the infinite cluster at the percolation threshold $p_c$ (bonds 7 and 8 are "dangling" and therefore are not visited by SAWs from $A$ to $B$). The fractal in Fig. 2c is a "two-dimensional" hierarchical lattice, and the one in Fig. 2d is a "three-dimensional" hierarchical lattice (these names relate to the minimal dimensions of Euclidean lattices on which these structures can be embedded). In Figs. 2e and 2f simple hierarchical lattices of two and four branches are illustrated (these hierarchical lattices are sometimes used to model the problem of directed SAWs[5, 6]).

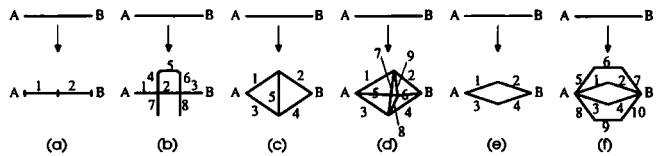


Fig. 2. Two stages of the iterative construction of the fractals: (a) One-dimensional lattice. (b) Mandelbrot–Given curve. (c) Two-dimensional hierarchical lattice. (d) Three-dimensional hierarchical lattice. (e) Simple lattice of two branches. (f) Simple lattice of two and three branches. The SAW enters the lattices at point $A$ and exits at point $B$. The bonds of each fractal are numbered for later use.

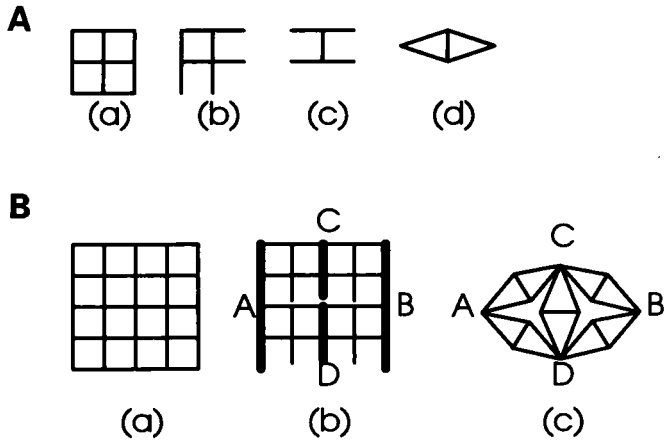


Fig. 3. (A) The translation of a two-dimensional square lattice to a hierarchical lattice: (a) The square lattice. (b) First-iteration renormalization cell. (c) A horizontal H-cell, which is the backbone of (b) for SAWs from left to right. (d) Connecting the endpoints in each side results in the two-dimensional hierarchical lattice. (B) Second stage of the two-dimensional hierarchical lattice: (a) The square lattice. (b) Separation into vertices. (c) Two-dimensional hierarchical lattice.

The hierarchical lattices are used to model SAWs on regular Euclidean lattices, as explained using Fig. 3A. In this figure, a two-dimensional square lattice is presented [Fig. 3A(a)]. A SAW starts at any point on the lattice's left edge and terminates at any point on its right edge. The exact locations of the starting point and of the ending point on the edges are irrelevant for the SAW fractal dimension. Following this, the lattice can be replaced by a horizontal "H-cell" [Fig. 3A(c)], which is the backbone of the lattice first-iteration renormalization cell [Fig. 3A(b)]. Connecting the two edges of this H-cell clearly does not have any effect on the SAW, and this translates the H-cell to the hierarchical lattice [Fig. 3A(d)]. The H-cell has been successfully used to renormalize various properties of random and percolating lattices.[7,8]

Another stage of the construction of the two-dimensional hierarchical lattice is illustrated in Fig. 3B. In Fig. 3B(b) the lattice is separated into two halves (top and bottom), and the bold lines indicate edges that are unified to one vertex in Fig. 3B(c).

## 3. THE ANALYTICAL METHOD

We define the free energy of a SAW on a fractal structure as follows. Consider a fractal of the $n$th generation and (horizontal) linear size $L = b^n$ ($b = 2$ for all the lattices presented in Fig. 2). We wish to study

the behavior of a SAW on a random environment, and therefore we assign a random energy $\varepsilon_i$ out of an initial distribution for each bond $i$. The statistical weight associated with each step of the SAW is $x_i = \exp[-(\varepsilon_i - \mu)/kT]$, where $kT$ is the thermal energy and $\mu$ is the chemical potential per single step. $x$ is sometimes called a "fugacity" per single step, generalizing the usual definition of fugacity $x = \exp(\mu/kT)$. We choose to work in a grand-canonical ensemble, in which both ends of the SAW are fixed to the edges of the lattice. Therefore the partition function is the sum over all legitimate edge-to-edge SAWs of all lengths $N$ of the products of statistical weights,

$$Z_n = \sum_{\text{SAWs}} \prod_{i=1}^{N} e^{(-\varepsilon_i + \mu)/kT} = \sum_{\text{SAWs}} \prod_{i=1}^{N} x_i \tag{3.1}$$

In generation zero (the upper line of Fig. 2), the lattice contains only one bond and therefore the partition function for this generation is $Z_0 = x$. If we replace this bond by a renormalized bond (after $n$ iterations), then it is clear that $Z_n$ fulfills the role of an effective renormalized fugacity per step on the $n$th generation structure: $Z_{n+1}$ is obtained from Eq. (3.1) for a single-iteration structure (like those in Fig. 2), with $x_i$ replaced by $Z_n(i)$.

In our model, the bond energy $\varepsilon_i$ is a random variable with a distribution function $g(\varepsilon)$. We prefer to work with $x$ as the random variable and therefore we define a distribution function $p(x)$. The transformation from $g(\varepsilon)$ to $p(x)$ follows from $g(\varepsilon)|d\varepsilon| = p(x(\varepsilon))|dx|$. Therefore,

$$p(x) = g(\varepsilon)\left|\frac{d\varepsilon}{dx}\right| = \frac{kT}{x} g\{\mu - kT \cdot \ln(x)\} \tag{3.2}$$

In the following sections we will use the real-space renormalization group (RSRG) to obtain recursion relations for the moments of the partition function $\langle Z'^k \rangle$ of a SAW of the next generation as functions of the moments $\langle Z \rangle, \langle Z^2 \rangle, \ldots, \langle Z^k \rangle$ in the present generation, where the $k$th moment of the present generation partition function is defined by

$$\langle Z^k \rangle = \int Z^k p(Z)\, dZ \tag{3.3}$$

where on the RHS, $p(Z)$ represents the distribution function of $Z$ for any bond in the present generation.

The recursion relations for the first two moments will be discussed in Section 4. These relations immediately yield a recursion relation for the variance, and will therefore enable us to check whether the variance flows toward increasing or decreasing disorder under the RSRG iterations. The

flow of higher cumulants under RSRG iterations will be discussed in Section 5. Analysis of all the cumulants will enable us to check whether the nonrandom fixed point (when all the bonds have the same value of $Z$) is stable against small disorder.

## 4. WEAK-DISORDER–STRONG-DISORDER PHASE TRANSITION

### 4.1. The Fugacity Distribution Function Flow on the One-Dimensional Lattice

We will first demonstrate the analysis of the distribution function flow in the simplest case, which is the one-dimensional lattice. The RSRG cell in this case consists of two sequential bonds, hence under a RSRG iteration the cell fugacity is equal to $Z' = Z_1 Z_2$. The distribution function after one iteration $p'(Z')$ is the sum over all the products of the basic distribution functions $p(Z_i)$ of the two bonds $(i = 1, 2)$, with the constraint that $Z' = Z_1 Z_2$,

$$p'(Z') = \int p(Z_1)\, p(Z_2) \cdot \delta(Z' - Z_1 Z_2)\, dZ_1\, dZ_2 \tag{4.1}$$

We now express the $k$th moment $\langle Z'^k \rangle$ after a RSRG iteration as a function of the $\langle Z^k \rangle$. Straightforward substitution then yields

$$\langle Z'^k \rangle = \int Z'^k p'(Z')\, dZ' = \int Z_1^k Z_2^k p(Z_1)\, p(Z_2)\, dZ_1\, dZ_2 = \langle Z^k \rangle^2 \tag{4.2}$$

for $k = 1, 2, 3, \ldots$.

For a nonrandom environment, in which the bond energy $\varepsilon$ is constant, the system's fixed point satisfies $Z' = Z$. Thus the initial bond fugacity equals the renormalized cell fugacity, and this leads to self-similarity: the system resembles itself at any length scale due to the inability to recognize this scale by the value of fugacity. In the case of a random environment, a fixed point in the simplified sense should satisfy an equality of all the moments, namely $\langle Z'^k \rangle = \langle Z^k \rangle$ for all $k$. Equation (4.2) thus yields three fixed points, $\langle Z^k \rangle^* = 0$, $\langle Z^k \rangle^* = 1$, or $\langle Z^k \rangle^* = \infty$. The fixed points with $\langle Z^k \rangle^* = 0$ or $\langle Z^k \rangle^* = \infty$ for all $k$ are trivial and not interesting. Thus, we choose for $k = 1$ the nontrivial value $\langle Z \rangle^* = 1$. At this fixed value, we can then use Eq. (4.2) to obtain the variance of the fugacity distribution function, $v' \equiv \mathrm{var}'(Z')$,

$$v'(Z') = \langle Z'^2 \rangle - \langle Z' \rangle^2 = v(Z) \cdot [2 + v(Z)] \tag{4.3}$$

where the right-hand side was found after substituting the fixed-point value $\langle Z\rangle^* = 1$. The expression for $v(Z)$ is always nonnegative and therefore $v'(Z') \geqslant v(Z)$, with an equality valid only if $v(Z) = 0$. The latter case corresponds to the nonrandom-case fixed point, where $\langle Z\rangle^* = 1$ and $v^*(Z^*) = 0$. The inequality implies that when the initial variance is positive, the renormalized variance "flows" to infinity, and there exists no fixed point with a finite var$(Z)$. The variance in this case diverges rapidly, no matter how small the initial disorder is, toward a point which Le Doussal and Machta[4] denoted as "strong disorder" (SD). The flow away from the nonrandom fixed point can be quantitatively characterized by a critical exponent $\lambda$, which is defined as follows: near this fixed point, where $\langle Z\rangle = 1$ and var$(Z) = 0$, we have $v' \approx 2v = b^\lambda v$, so that $\lambda = 1$ for the one-dimensional lattice (the rescale factor $b$ is equal to 2 for this example). After performing $n$ RSRG iterations, if the disorder remains weak, the variance flows toward $v'^{(n)} \sim b^{n\lambda} v = L^\lambda v$. We can therefore say that $\lambda$ describes the growth of the effective variance with the linear scale $L$. As discussed in Section 5, similar arguments can be used for all higher cumulants.

## 4.2. The Distribution and the Average Flow on a General Lattice

We will now expand the analysis presented in the previous section to the case of any arbitrary hierarchical lattice. In order to avoid the need to write down heavy expressions, we first define several notations. To demonstrate these notations, each one of them will be accompanied by its implementation to the Mandelbrot–Given curve (Fig. 2b).

We first define the product of the basic distribution function and the differential elements over all the bonds $i$ of the RSRG cell of the hierarchical lattice, $\mathscr{D}Z \equiv \prod_i [p(Z_i)\, dZ_i]$. We next define the RSRG cell fugacity $Z'$ as a function of the basic fugacities $Z_i$, $\mathscr{Z}'\{Z_i\}$. We also define the notation $\mathfrak{R}(Z)$, which is the RSRG transformation for the nonrandom case, namely $Z' = \mathfrak{R}(Z)$.

For the Mandelbrot–Given curve the explicit implementations of these notations are

$$\begin{aligned}\mathscr{D}Z &\equiv \prod_i [p(Z_i)\, dZ_i] \\ &= p(Z_1)\, p(Z_2)\, p(Z_3)\, p(Z_4)\, p(Z_5)\, p(Z_6)\, p(Z_7)\, p(Z_8) \\ &\quad \times dZ_1 dZ_2 dZ_3 dZ_4 dZ_5 dZ_6 dZ_7 dZ_8 \qquad (4.4a)\end{aligned}$$

$$\mathscr{Z}'\{Z_i\} = Z_1 Z_2 Z_3 + Z_1 Z_4 Z_5 Z_6 Z_3 \qquad (4.4b)$$

and

$$\mathfrak{R}(Z) = Z^3 + Z^5 \tag{4.4c}$$

We can now obtain the distribution function $p'(Z')$ after one RSRG iteration,

$$p'(Z') = \int \delta(Z' - \mathscr{Z}'\{Z_i\})\, \mathscr{D}Z \tag{4.5}$$

Note that the integral over the dangling bonds 7 and 8 of Fig. 2b reduces to unity, since a SAW from $A$ to $B$ cannot access those bonds. The renormalized distribution function immediately yields an expression for the renormalized average $\langle Z' \rangle$,

$$\langle Z' \rangle = \int Z' \cdot p'(Z')\, dZ' = \int \mathscr{Z}'\{Z_i\}\, \mathscr{D}Z = \mathfrak{R}(\langle Z \rangle) \tag{4.6}$$

meaning that the fugacity's average transformation is identical to the fugacity's transformation in the nonrandom case. We note that this simple result is an outcome of the fact that the fugacity recursion function is a sum of products, in each of which every bond is represented by a single factor $Z_i$. This is special to this case and cannot be applied to a general problem (e.g., electrical currents in a resistor network). Following this result, the fugacity's average fixed point is identical to that of the nonrandom case,

$$\langle Z \rangle^* = \mathfrak{R}(\langle Z \rangle^*) \tag{4.7}$$

Thus, $\langle Z \rangle^* = Z^*$, where $Z^*$ is the "nonrandom" fixed-point value. This is the only nontrivial fixed point value of $\langle Z \rangle$ for our class of problems.

Obtaining a similar expression for the second moment is a little more complicated. When the cell fugacity is raised to the second power, the expression which is obtained contains mixed elements, and therefore a special calculation has to be applied for each one of the lattices separately.

### 4.3. The Flow of the Variance in the $v'$–$v$ Plane and the Weak-Disorder Decay Exponent

In the forthcoming sections, we will analyze the flow of the variance on the lattices presented in Fig. 2. We will first fix the average of the distribution at the fixed point $\langle Z \rangle = Z^*$ and then study the dependence of the variance in the next generation $v'$ as a function of the present generation's $v$. In the nonrandom case, $v = 0$ and then $v'$ is also equal to zero.

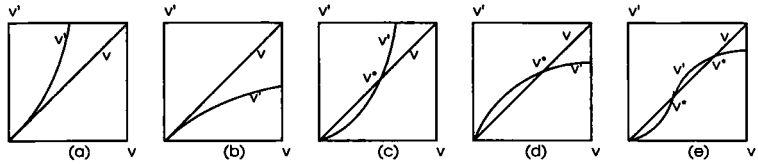


Fig. 4. Various options of the variance flow in the $v'$–$v$ plane: (a) For every positive $v$, $v'$ always satisfies $v' > v$. (b) For every positive $v$, $v'$ always satisfies $v' < v$. (c) There is a value $v^*$ for which $v' = v$, below it $v' < v$, and above it $v' > v$. (d) There is a value $v^*$ for which $v' = v$, below it $v' > v$, and above it $v' < v$. (e) There are several values $v^*$ for which $v' = v$.

Therefore, one might expect the function $v'(v)$ to have one of the shapes shown in Fig. 4.

We will now analyze the recursion relation for the second moment $\langle Z'^2 \rangle$ and show that among these five possibilities of Fig. 4, only Figs. 4a and 4c are possible. The recursion relation for the second moment is

$$\langle Z'^2 \rangle = \int Z'^2 \cdot p'(Z')\, dZ'$$

$$= \int \mathscr{Z}'^2\{Z_i\}\, \mathscr{D}Z = \mathsf{P}_m(\langle Z^2 \rangle) = \sum_{i=0}^{m} a_i(Z^*)\langle Z^2 \rangle^i \qquad (4.8)$$

where $\mathsf{P}_m(\langle Z^2 \rangle)$ is a polynomial of order $m$ in $\langle Z^2 \rangle$ with coefficients $a_i(z^*)$, and $m$ is the longest SAW length on a renormalization cell ($m = 2, 5, 3, 4, 2, 3, 8$ for Figs. 2a–2g, respectively). Since $\mathscr{Z}'\{Z_i\}$ is a sum of positive terms, all the coefficients $a_i$ of the polynomial are nonnegative. We can now construct a general recursion relation for $v'$ by subtracting the value $(Z^*)^2 = \sum a_i(Z^*)^{2i}$ [this equality follows from substituting the nonrandom distribution $p(Z) = \delta(Z - Z^*)$ into (4.8)] from both sides of (4.8), and substituting $\langle Z^2 \rangle = v + (Z^*)^2$ into the right-hand side. This results in

$$v' = \sum_{i=0}^{m} a_i[v + (Z^*)^2]^i - \sum_{i=0}^{m} a_i(Z^*)^{2i}$$

$$= \sum_{i=1}^{m} \left[ \sum_{j=1}^{m} a_j(Z^*)^{2(j-i)} \binom{j}{i} \right] v^i \equiv \sum_{i=1}^{m} b_i v^i \qquad (4.9)$$

where all the coefficients $b_i$ are nonnegative since they are sums of nonnegative terms, and $b_0 = 0$ to satisfy the demand for the nonrandom case $v'(v = 0) = 0$. Due to the fact that all the $b_i$'s are nonnegative, the function $v'(v)$ and all its derivatives are monotonically increasing. The behavior of $v'$

in the limits $v \to 0$ and $v \to \infty$ is also derived from (4.9): for $v \to 0$, $v' \sim v$, while for $v \to \infty$, $v' \sim v^m$.

Only the plots Figs. 4a and 4c are consistent with the above results, and each one of them represents a different scenario of the variance flow. If Fig. 4a is valid for a certain lattice, any amount of initial disorder is relevant, and it will always flow toward increasing disorder. If Fig. 4c is valid, initial disorder corresponding to $v > v^*$ causes the distribution function to flow toward strong disorder. However, if $v < v^*$, the system has one of the following behaviors: (1) if all the higher cumulants also flow to zero, the initial disorder is irrelevant and the distribution function flows toward the nonrandom case, or (2) if any higher cumulant diverges, the distribution function is centered around $Z^*$ with a zero width but with an infinite tail (this tail, if exists, is not important regarding the average and the variance, but it may affect higher cumulants). The flow of the higher cumulants is discussed in Section 5, and it is shown there that for lattices for which the variance decays, there is a region of sufficiently weak disorder in which all the higher cumulants decay as well.

All of the above analysis was carried out without making any assumption concerning the initial distribution, and the specific expressions of the variance depended only on the type of the lattice. Therefore we will now suggest a criterion that will assist in determining whether or not a specific lattice has a weak-disorder–strong-disorder phase transition. In the strong-disorder regime, for sufficiently large $v$, the renormalized variance $v'$ will always be larger than $v$, and therefore a transition from the regime $v' < v$ to the regime $v' > v$ will occur if the condition $v'(v) < v$ is valid in the neighborhood of $v \to 0$. As discussed above, we can define a critical exponent $\lambda$, which we call the "disorder decay exponent", through the relation

$$\left.\frac{\partial v'}{\partial v}\right|_{v=0} = \sum_{i=1}^{m} i a_i (Z^*)^{2(i-1)} \equiv b^{\lambda} \tag{4.10}$$

which defines $\lambda$ to be equal to

$$\lambda = \frac{\log\left(\partial v'/\partial v|_{v=0}\right)}{\log(b)} \tag{4.11a}$$

If $\lambda > 0$, i.e., $b^{\lambda} > 1$, then $v'(v) > v$ for all $v$, and there is no "weak–strong" transition. [See Fig. 4a]. On the other hand, if $\lambda < 0$, then $v'$ "flows" toward zero for small $v$ and toward infinity for large $v$, allowing for the weak–strong transition and for a nontrivial fixed point $v^*$ separating the above two flow directions. [See Fig. 4c].

Since we are interested in the flow of the variance when $\langle Z \rangle = Z^*$, we can add the constant $(Z^*)^2$ to both $v$ and $v'$ in the derivative in (4.11a), and obtain an equivalent expression for $\lambda$,

$$\lambda = \log\left( \left. \frac{\partial \langle Z'^2 \rangle}{\partial \langle Z^2 \rangle} \right|_{\langle Z^2 \rangle = Z^{*2}} \right) \Big/ \log(b) \tag{4.11b}$$

Let us now give a graphical interpretation to the value of $b^\lambda$ by looking at the $a_i$. These are defined in (4.8) as the coefficients of $\langle Z^2 \rangle^i$ in the expression for $\langle Z'^2 \rangle$. Executing the integral (4.8) is analogous to drawing up diagrams for all the closed loops that start from the RSRG cell's origin, perform a self-avoiding-walk pattern to the second edge of the cell, and returning to the origin in another self-avoiding-walk pattern. In each such loop, there are $n_1$ bonds that are passed once, each contributing a factor of $\langle Z \rangle = Z^*$ to the term. Each loop also has $n_2$ bonds that are passed twice, each contributing a factor of $\langle Z^2 \rangle$. The loop's total length is equal to $l = n_1 + 2n_2$ (the summation index $i$ is actually equal to $n_2$). The expression for $\langle Z'^2 \rangle$ is a sum over all the contributions of the various loops.

This approach is demonstrated for the Mandelbrot–Given curve in Fig. 5. In this figure, all the four different loops start at the origin $A$, pass through the second edge $B$, and return to $A$. A direction is associated with each loop, meaning that each loop is actually counted twice (apart from the totally self-overlapping loops in Figs. 5a and 5b). The contribution of each loop to the expression of $\langle Z'^2 \rangle$, as well as the parameters $l, n_1$ and $n_2$ of each loop, are written at the top of the figure.

Following this graphical approach, we can replace the summation in (4.10) by summing over all the loops in RSRG cell, and obtain the expression

$$b^\lambda = \sum_{i=1}^{m} i a_i (Z^*)^{2(i-1)} = \sum_{\text{loops}} n_2 (Z^*)^{n_1} (Z^*)^{(2n_2-1)} = \sum_{\text{loops}} n_2 (Z^*)^{l-2} \tag{4.12}$$

The use of Eq. (4.12) can be demonstrated for the one-dimensional lattice (Fig. 2a): in that case one has only one loop, with $n_2 = 2$, yielding $b^\lambda = 2$ and $\lambda = 1$ ($Z^* = 1$ for this lattice). Therefore on this lattice $v \sim L$. For a

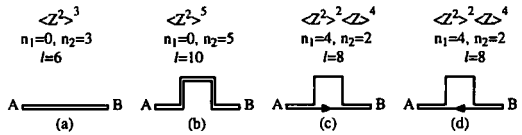


Fig. 5. A graphical approach for the calculation $\langle Z'^2 \rangle$.

general lattice, Eq. (4.12) implies that $b^\lambda$ depends on several geometrical properties of the lattice. These properties and their contribution to the value of $b^\lambda$ will be discussed in Section 4.7.

## 4.4. The Flow of the Variance on the Mandelbrot–Given Curve

We now analyze the flow of the variance on the MG curve, fixing $\langle Z \rangle$ at the nonrandom fixed point $Z^*$. Following Eqs. (4.4c) and (4.7), this fixed point obeys the equation $\langle Z \rangle = \langle Z \rangle^3 + \langle Z \rangle^5$, whose nontrivial solution is $\langle Z \rangle = Z^* = 0.7861...$ .

In order to calculate $\lambda$, we can simply use the graphical approach that was presented in Section 4.3. Substituting the parameters listed in Fig. 5 and summing (4.12) over all the loops yields

$$b^\lambda = 3Z^{*4} + 5Z^{*8} + 2Z^{*6} + 2Z^{*6} = 2.8197...$$

i.e., $\lambda = \log(2.8197)/\log(2) = 0.9436...$ . We can also obtain an explicit expression for the flow of the variance $v$ by following Eqs. (4.8) and (4.9),

$$\langle Z'^2 \rangle = \int Z'^2 \cdot p'(Z')\, dZ'$$

$$= \int \mathscr{Z}'^2\{Z_i\}\, \mathscr{D}Z = \langle Z^2 \rangle^3 + \langle Z^2 \rangle^5 + 2\langle Z^2 \rangle^2 \langle Z \rangle^4 \quad (4.13)$$

and therefore

$$\begin{aligned} v' &= (Z^{*2} + v)^3 + (Z^{*2} + v)^5 + 2Z^{*4}(Z^{*2} + v)^2 - Z^{*2} \\ &= v^5 + 5Z^{*2}v^4 + (1 + 10Z^{*4})v^3 + (3Z^{*2} + 10Z^{*6} + 2Z^{*4})v^2 \\ &\quad + (3Z^{*4} + 5Z^{*8} + 4Z^{*6})v \end{aligned} \quad (4.14)$$

As expected, this relation immediately yields a fixed point at the value $v^* = 0$. If any disorder exists in the system ($v > 0$), the variance flows toward increasing disorder, no matter how weak the initial disorder was. For weak disorder, $v'$ increases as $v' = b^\lambda v$. Since $\lambda > 0$, the variance flow for the MG curve resembles Fig. 4a, with no nontrivial fixed point of the variance and no weak-disorder–strong-disorder transition.

## 4.5. The Flow of the Variance on the Hierarchical Lattices

We will now analyze the variance flow on the hierarchical lattices in Figs. 2c (the two-dimensional lattice) and 2d (the three-dimensional lattice).

For the lattice in Fig. 2c, the cell fugacity recursion relation is

$$\mathscr{Z}'\{Z_i\} = Z_1Z_2 + Z_3Z_4 + Z_1Z_5Z_4 + Z_3Z_5Z_2 \tag{4.15}$$

The recursion relation for the average is $\langle Z' \rangle = 2(\langle Z \rangle)^2 + 2(\langle Z \rangle)^3$. This relation leads to an equation for the fixed point, $\langle Z \rangle^* = 2(\langle Z \rangle^*)^2 + 2(\langle Z \rangle^*)^3$, with the nontrivial solution $\langle Z \rangle = Z^* = 0.3660...$. Substituting $\mathscr{Z}'\{Z_i\}$ into the expression for $\langle Z'^2 \rangle$ results in

$$\begin{aligned}\langle Z'^2 \rangle &= \int \mathscr{Z}'^2\{Z_i\}\, \mathscr{D}Z \\ &= 2\langle Z^2 \rangle^2 + 2\langle Z^2 \rangle^3 + 2\langle Z \rangle^4 + 8\langle Z^2 \rangle \langle Z \rangle^3 + 2\langle Z^2 \rangle \langle Z \rangle^4 \end{aligned} \tag{4.16a}$$

and therefore

$$\begin{aligned} v' &= 2(Z^{*2} + v)^2 + 2(Z^{*2} + v)^3 + 2Z^{*4} + 8Z^{*3}(Z^{*2} + v) \\ &\quad + 2Z^{*4}(Z^{*2} + v) - Z^{*2} \\ &= 2v^3 + (2 + 6Z^{*2})v^2 + (4Z^{*2} + 8Z^{*4} + 8Z^{*3})v \end{aligned} \tag{4.16b}$$

Again, the flow in the $v'$–$v$ plane is of the shape of Fig. 4a, with no nontrivial fixed point. As in the case of the MG curve, the only fixed point of the variance is the nonrandom case $v = 0$, and any amount of initial disorder causes the system to flow toward strong disorder. We also find

$$b^\lambda = 4Z^{*2} + 8Z^{*3} + 8Z^{*4} = 1.0718...$$

and $\lambda = \ln(1.0718)/\ln(2) = 0.1000...$, meaning that for this "two-dimensional" lattice the disorder increases much slower as a function of $L$ compared with the MG curve.

For the "three-dimensional" hierarchical lattice (Fig. 2d), the recursion relation for $\mathscr{Z}'\{Z_i\}$ is very heavy and contains 15 terms:

$$\begin{aligned}\mathscr{Z}'\{Z_i\} &= Z_1Z_2 + Z_3Z_4 + Z_5Z_6 + Z_1Z_7Z_4 + Z_1Z_9Z_6 + Z_3Z_7Z_2 \\ &\quad + Z_3Z_8Z_6 + Z_5Z_8Z_4 + Z_5Z_9Z_2 + Z_1Z_7Z_8Z_6 + Z_1Z_9Z_8Z_4 \\ &\quad + Z_3Z_7Z_9Z_6 + Z_3Z_8Z_9Z_2 + Z_5Z_8Z_7Z_2 + Z_5Z_9Z_7Z_4 \end{aligned} \tag{4.17}$$

Thus, $\langle Z' \rangle = 3\langle Z \rangle^2 + 6\langle Z \rangle^3 + 6\langle Z \rangle^4$. This relation leads to an equation for the fixed point, $Z^* = 3Z^{*2} + 6Z^{*3} + 6Z^{*4}$, with the nontrivial solution

$\langle Z\rangle^* = 0.2178\ldots$. Substituting $\mathscr{Z}'\{Z_i\}$ into Eq. (4.8) leads to a long but straightforward calculation, with the result

$$\begin{aligned}\langle Z'^2\rangle = {} & 6\langle Z^2\rangle^4 + 6\langle Z^2\rangle^3 + [3 + 36\langle Z\rangle^3 + 18\langle Z\rangle^4]\langle Z^2\rangle^2 \\ & + [24\langle Z\rangle^3 + 42\langle Z\rangle^4 + 24\langle Z\rangle^5 + 12\langle Z\rangle^6]\langle Z^2\rangle \\ & + [6\langle Z\rangle^4 + 12\langle Z\rangle^5 + 24\langle Z\rangle^6 + 12\langle Z\rangle^7] \qquad (4.18a)\end{aligned}$$

or alternatively

$$\begin{aligned}v' = {} & 6v^4 + (6 + 24Z^{*2})v^3 + (3 + 18Z^{*2} + 36Z^{*3} + 54Z^{*4})v^2 \\ & + (6Z^{*2} + 24Z^{*3} + 60Z^{*4} + 96Z^{*5} + 72Z^{*6})v \qquad (4.18b)\end{aligned}$$

For this lattice

$$b^\lambda = (6Z^{*2} + 24Z^{*3} + 60Z^{*4} + 96Z^{*5} + 72Z^{*6}) = 0.7223$$

and $\lambda \doteq \ln(0.7223)/\ln(2) = -0.4693\ldots$. Since $\lambda < 0$, the flow has a nontrivial fixed point, which is numerically found to be at $v^* = 0.0581\ldots$ (as shown in Fig. 6).

The new nontrivial fixed point that was found is unstable: every initial $v$ which is smaller or larger than $v^*$ will flow to zero or toward strong disorder, respectively. This is exactly the analytical presentation to the phase transition that was observed by Le Doussal and Machta: if the average fugacity equals the nonrandom fugacity's fixed point, any weak initial disorder will disappear when we look at the SAW on a large length scale. In contrast, a disorder whose variance is larger than $v^*$ will diverge toward strong disorder. In Section 5 we will show that in the weak-disorder regime higher cumulants decay faster, meaning that for lattices with $\lambda < 0$ there is a region where all the cumulants decay and weak disorder is irrelevant. Numerically it comes out that the amount of disorder that can be considered "weak" is actually not so small; in the case of the lattice studied

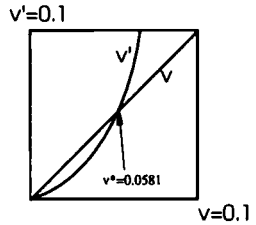


Fig. 6. The flow of the variance at the average fixed point $\langle Z\rangle = Z^*$ on the three-dimensional hierarchical lattice.

here, the standard deviation at the phase transition is equal to $\sigma = \sqrt{0.0581} = 0.2410...$, which is larger than the fixed point of the average, $\langle Z \rangle^* = 0.2178...$ .

## 4.6. "Two-Dimensional" Fractals Which Are Stable or Marginal to Weak Disorder

As we mentioned earlier, Le Doussal and Machta[4] observed that the stability to disorder was related to the dimensionality of the embedding Euclidean lattice; on lattices that they called "two dimensional" the flow was toward strong disorder, while on "three-dimensional" lattices weak disorder was irrelevant. We will now examine the lattices presented in Figs. 2e and 2f, and show that although their stability to weak disorder is determined by some geometric characteristics of the structures, these are not simply related to the dimensions of the embedding Euclidean lattices.

For the lattice in Fig. 2e, the recursion for the average is $\langle Z' \rangle = 2\langle Z \rangle^2$, thus $Z^* = 0.5$. It is most simple to calculate $b^\lambda$ for this lattice using the graphical approach explained in Section 4.3. The open loops (i.e., the loops which contain no bonds that are being passed twice) do not contribute to the summation in Eq. (4.12), since they have $n_2 = 0$. The only contribution then comes from the totally self-overlapping loops (i.e., the loops for which all the bonds are being passed twice). The expression for $b^\lambda$ is then

$$b^\lambda = 4Z^{*2} = 1 \tag{4.19}$$

Thus $\lambda = 0$, meaning that for this fractal the slope of the $v'(v)$ plot at $v = 0$ is exactly equal to 1. Therefore this is a marginal case between the existence and nonexistence of a weak-disorder–strong-disorder phase transition. Due to the marginal behavior, it is interesting to look at the second term for $v'$ in the weak-disorder regime, which is found to be exactly $v' = v + 2v^2$. If the initial disorder (in generation zero) is $v_0$, taking the first correction term after $n$ RSRG iterations yields

$$v \approx v_0 + 2n{v_0}^2 = v_0 + 2 \log_b(L){v_0}^2 \tag{4.20}$$

As stated before, this approximation is valid only in the weak-disorder regime, $v_0 \log_b(L) \ll 1$. However, it does show that the nonrandom fixed point $v = 0$ is unstable, and that $v$ flows toward strong disorder [this was expected since $v'(v)$ and all its derivatives are monotically increasing, as in Fig. 4a].

Regarding the fractal of Fig. 2f, the recursion for the average is $\langle Z' \rangle = 2\langle Z \rangle^2 + 2\langle Z \rangle^3$, thus $Z^* = 0.3660...$ . Applying (4.12) to it yields

$$b^\lambda = 4Z^{*2} + 6Z^{*4} = 0.6435... \tag{4.21}$$

**Table I. The Disorder Decay Exponent λ for Several Lattices**

| Lattice | Figure | $Z^*$ | $\lambda$ |
|---|---|---|---|
| One-dimensional lattice | 2a | 1 | 1 |
| Mandelbrot–Given curve | 2b | 0.7862... | 0.9436... |
| Two-dimensional hierarchical lattice | 2c | 0.3660... | 0.1000... |
| Three-dimensional hierarchical lattice | 2d | 0.2178... | −0.4693... |
| Simple lattice of two branches | 2e | 1/2 | 0 |
| Simple lattice of four branches | 2f | 0.3660... | −0.6360... |

resulting in a negative $\lambda = \ln(0.6435)/\ln(2) = -0.6360...$. Therefore, a nontrivial fixed point $v^*$ and a weak-disorder–strong-disorder transition exists for this fractal.

## 4.7. The Weak-Disorder Exponent and the Geometrical Properties Which Influence λ

To summarize this section, we give in Table I the values of the disorder decay exponents for the lattices studied in this paper.

These results imply that there is no trivial dependence of the value of $\lambda$ on the dimensionality of the embedding lattice, and that $\lambda$ is a rather complicated function of the geometry of each lattice. Looking at Eq. (4.12), we can identify two main factors derived from the lattice geometry which influence the value of $\lambda$. The first factor is the value of $Z^*$, which is indirectly influenced by the geometry through the renormalized partition function $Z'(Z)$: the greater is the number of minimal-length paths (i.e., two step lengths) in a renormalization cell, the smaller is $Z^*$. Since $Z^*$ is always smaller than 1, Eq. (4.12) implies that in order to have a small $\lambda$, the lattice should contain many of these paths.

The second factor which influences $\lambda$ concerns the loops which contain doubly passed bonds (i.e., those loops with $n_2 > 0$). Each such loop contributes a positive term to the summation in (4.12) and enlarges the value of $\lambda$. Lattices which contain many loops, or lattices which contain singly connected bonds, are therefore bad candidates to have a small value of $\lambda$ and a weak-disorder–strong-disorder transition. Let us explicitly examine the case of a lattice whose RSRG cell contains $n_{sc}$ singly connected bonds ($n_{sc} > 0$). For such a lattice, $n_2 \geqslant n_{sc}$ for all the loops, and thus we have a lower bound for (4.12)

$$b^{\lambda} = \sum_{\text{loops}} n_2 (Z^*)^{l-2} \geqslant n_{sc} \sum_{\text{loops}} (Z^*)^{l-2} = n_{sc} \left[ \sum_{\text{SAWs}} (Z^*)^{N-1} \right]^2 = n_{sc} \quad (4.22)$$

where the sum over the loops was replaced by the square of the sum over all the edge-to-edge SAWs on a RSRG cell (each of them containing $N$ steps), and $\sum_{\text{SAWs}}(Z^*)^{N-1}=1$ since $Z^*$ obeys the fixed-point equation $Z'=Z$ for the partition function in the nonrandom case, $Z'=\sum_{\text{SAWs}}Z^N$. Thus, Eq. (4.22) states that the absence of singly connected bonds is a necessary condition for a lattice to have stability against weak disorder.

The influence of the loops which contain doubly passed bonds is clearly seen when comparing the values of $\lambda$ between the fractals of Figs. 2c and 2f. The fixed point $Z^*$ and the total number of possible loops (16) are equal for both of them. However, only four loops in the fractal of Fig. 2f contain $n_2>0$ and contribute to $\lambda$, versus 14 contributing loops in the fractal of Fig. 2c. Therefore, $\lambda$ is much smaller for the former.

## 5. THE FLOW OF HIGHER CUMULANTS

In Section 4, we saw several lattices for which the nonrandom fixed point was stable against a finite small variance $v$. In this section, we will show that if on a certain lattice the variance flows to zero, then there is a region of sufficiently weak disorder in which *all* the higher cumulants flow to zero as well. Inside this region, the distribution itself flows toward a nonrandom function ($\delta$ function). The analysis carried out in this section is a generalization of the graphical approach presented in Section 4.3.

Defining

$$\langle Z'^k\rangle=\int \mathscr{Z}'^k\{Z_i\}\,\mathscr{D}Z \tag{5.1}$$

we now generalize our discussion of $k=2$. We start by defining at $k$-loop, as a path that starts at the origin and performs $k$ edge-to-edge SAWs from one edge to the other (and terminates at the origin if $k$ is even or at the second edge if $k$ is odd). In each $k$-loop, there are $n_i$ bonds that are passed $i$ times along the path, where $i=1, 2,..., k$. The $k$-loop's total length is $l_k=n_1+2n_2+\cdots+kn_k$. Executing the integral (5.1) is then equivalent to summing over all the $k$-loops,

$$\langle Z'^k\rangle=\sum_{k\text{-loops}}\langle Z^k\rangle^{n_k}\langle Z^{k-1}\rangle^{n_{k-1}}\cdots\langle Z\rangle^{n_1} \tag{5.2}$$

Assume a distribution function whose average is $Z^*$ and all the cumulants $C_2, C_3,..., C_{k-1}$ flow to zero, meaning that

$$\langle Z^2\rangle=Z^{*2},\qquad \langle Z^3\rangle=Z^{*3},...,\qquad \langle Z^{k-1}\rangle=Z^{*k-1}$$

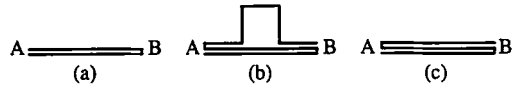


Fig. 7. Example of a parent and its children on the MG curve: (a) The two-loop parent, (b, c) its two three-loop children.

We wish to study the flow of the $k$th cumulant $C_k$, and define the exponent $\lambda_k$ which measures the decay or growth of $C_k$ with respect to the lattice linear size for a weak disorder (e.g., $\lambda_2$ is identical to the previously defined $\lambda$). Generalizing Eq. (4.12), this assumption yields

$$b^{\lambda_k} = \left.\frac{\partial C'_k}{\partial C_k}\right|_{C_k=0} = \left.\frac{\partial \langle Z'^k \rangle}{\partial \langle Z^k \rangle}\right|_{\langle Z^k \rangle = Z^{*k}} = \sum_{k\text{-loops}} n_k (Z^*)^{l_k - k} \tag{5.3}$$

Each $k$-loop can be constructed by sequentially performing a $(k-1)$-loop, which will be called a "parent," and an additional one-loop (a one-loop is actually an edge-to-edge SAW). The $k$-loop which is created by the combination of these two will be called a "child." An example of a two-loop parent and its two three-loop children on the MG curve is depicted in Fig. 7.

Thus, the sum in (5.3) can be separated into a sum over all the parents, where each term representing a parent contains a sum over all its children,

$$\begin{aligned} b^{\lambda_k} &= \sum_{(k-1)\text{-loops}} \sum_{1\text{-loops}} n_k (Z^*)^{l_k - k} \\ &= \sum_{(k-1)\text{-loops}} n_{k-1} (Z^*)^{l_{k-1} - (k-1)} \sum_{1\text{-loops}} \frac{n_k}{n_{k-1}} (Z^*)^{l_1 - 1} \end{aligned} \tag{5.4}$$

For a given parent, a child will have $n_k$ equal to $n_{k-1}$ only if all the parent's bonds that were passed $n_{k-1}$ times are passed also by the continuing one-loop. In other cases $n_k < n_{k-1}$. Therefore $n_k/n_{k-1} \leqslant 1$. Thus, there is an upper bound to (5.4),

$$\begin{aligned} b^{\lambda_k} &\leqslant \sum_{(k-1)\text{-loops}} n_{k-1} (Z^*)^{l_{k-1} - (k-1)} \sum_{1\text{-loops}} (Z^*)^{l_1 - 1} \\ &= \sum_{(k-1)\text{-loops}} n_{k-1} (Z^*)^{l_{k-1} - (k-1)} \equiv b^{\lambda_{k-1}} \end{aligned} \tag{5.5}$$

with the equality valid only if $n_k = n_{k-1}$ for all the pairs of parents and children, a condition which is obeyed only for the one-dimensional lattice (Fig. 2a). Again, we used

$$\sum_{1\text{-loops}} (Z^*)^{l_1 - 1} = 1$$

since $Z^*$ obeys the fixed-point equation $Z' = Z$ for the partition function in the nonrandom case ($Z' = \sum_{\text{SAWs}} Z^N$, and $N$ is equivalent to $l_1$). The result (5.5) states that for every hierarchical lattice, $\lambda_k < \lambda_{k-1}$ for all $k$'s, meaning that in a weak-disorder regime higher cumulants decay faster. The strong significance of this statement is that all the cumulants of a fractal for which $\lambda \equiv \lambda_2 < 0$ decay to zero for sufficiently weak disorder. Therefore, in order to understand the fractal's behavior in weak disorder, one only has to study the flow of the variance. However, the disorder could be strong enough so that all the cumulants $C_2, C_3, \ldots, C_{k-1}$ decay to zero, but the initial value of $C_k$ is large, so that $C_k$ increases under iterations. The divergence of $C_k$ is directly associated with a divergence of $\langle Z^k \rangle$. Since $Z$ is a positive random variable, higher moments than $k$ will diverge even stronger. Therefore, all the cumulants higher than $k$ will also diverge, and the distribution of the partition functions will flow toward a peculiar shape centered around $Z^*$, with a zero width and an infinite tail of negligible weight [an example of such a distribution is $p(Z) = \alpha\delta(Z - Z^*) + (1-\alpha)\,\delta(Z - Z_1)$, with $\alpha \to 1$, $Z_1 \to \infty$, $(1-\alpha)\,Z_1^2 \to 0$, and $(1-\alpha)\,Z_1^n \to c$ ($n > 2$ and $0 < c < \infty$)]. Another possible scenario in which the distribution flows toward this shape is that all the cumulants lower than $k$ flow to zero, $C_k$ flows to $C_k^*$, and all the higher cumulants diverge. However, we note that $\lambda_k$ measures the divergence of $C_k'$ only with respect to $C_k$. The full recursive expression for $C_k'$ also contains lower cumulants $C_i$ ($i < k$), which may cause $C_k$ to diverge even if $\lambda_k < 0$. We have not investigated this general case.

It is also interesting to check the flow of the high cumulants when $v$ is exactly equal to the nontrivial fixed point $v^*$. After studying the recursion relations for the lattices in Figs. 2d and 2f (for which there exists a nontrivial $v^*$), we found that for both of these lattices higher cumulants do not have a nontrivial fixed point and they diverge. In this case the flow of the distribution is toward a shape with a fixed average, a finite width, and an infinite tail.

## 6. CONCLUSIONS AND DISCUSSION

We established an analytical method to determine whether a weak-disorder–strong-disorder phase transition occurs on hierarchical lattices. If

such a transition exists, the nonrandom fixed point is stable against weak disorder. We examined several lattices, and found that the existence of this phase transition does not depend on the embedding lattices' Euclidean dimensionality, as was suggested in ref. 4, but rather on other geometrical features. Two of these features are (1) the value of $Z^*$, which is influenced by the number of minimal-length paths in a renormalization cell (these paths contribute to the stability to weak disorder), and (2) the complexity of the lattice, in the sense of how many loops containing doubly passed bonds exist in a RSRG cell (these loops reduce the stability to weak disorder). The actual stability to weak disorder depends on the balance between these two geometrical features. It was also shown that absence of singly connected bonds is a necessary condition for the stability against weak disorder.

We defined a critical exponent $\lambda$, which is negative when the nonrandom fixed point is stable against disorder, leading to a "weak–strong" transition. When $\lambda > 0$, one has only the "strong"-disorder behavior. For weak disorder, $\lambda$ describes how the effective partition function's variance $v$ depends on the lattice linear size $L$, $v \sim L^{\lambda}$. We calculated $\lambda$ for several hierarchical lattices, and found a lattice for which $\lambda = 0$, meaning that weak disorder is marginal. We also showed that the decay of higher cumulants is stronger than that of lower ones, namely $\lambda_k \leqslant \lambda_{k-1}$ for all $k$'s, where $\lambda_k$ is defined via the $L$ dependence of the $k$th cumulant, $C_k \sim L^{\lambda_k}$. This implies that in order to understand whether weak disorder grows or decays on a certain lattice, it is enough to study the flow of the variance.

In dilute systems at the percolation threshold,[9] even if all the bonds of the infinite percolation cluster are identical, disorder is generated by the randomness of the cluster configuration. Since the infinite cluster contains singly connected bonds, SAWs on this cluster have $\lambda > 0$, and weak disorder is relevant. Therefore we believe that the average-length SAW on percolation clusters is not controlled by the nonrandom fixed point, and thus that $D_{\text{saw}}$ at the percolation threshold differs from its value in the undiluted periodic lattice.

## ACKNOWLEDGMENTS

This paper was supported by the U.S.–Israel Binational Science Foundation (BSF), by the Israel Science Foundation, and by the German–Israeli Foundation (GIF).

## REFERENCES

1. P. G. de Gennes, *Scaling Concepts in Polymer Physics* (Cornell University Press, Ithaca, New York, 1979).

2. R. Rammal, G. Toulouse, and J. Vannimenus, *J. Math. Phys.* **19**(1):5 (1978).
3. Y. Shussman and A. Aharony, *J. Stat. Phys.* **80**:147 (1995).
4. P. Le Doussal and J. Machta, *J. Stat. Phys.* **64**:541 (1991).
5. B. Derrida and R. B. Griffiths, *Europhys. Lett.* **8**:116 (1989).
6. J. Cook and B. Derrida, *J. Stat. Phys.* **57**:89 (1989).
7. P. J. Reynolds, W. Klein, and H. E. Stanley, *J. Phys. C* **10**:L167 (1977).
8. A. Aharony *et al.*, *Physica A* **177**:260 (1991).
9. D. Stauffer and A. Aharony, *Introduction to Percolation Theory*, rev. 2nd ed. (Taylor and Francis, 1994).